

# Improvement of the Nafion–Polytetrafluoroethylene Membranes for Potential Direct Methanol Fuel Cell Use by Reduction of the Methanol Crossover

Haolin Tang, Mu Pan, Wan Zhaohui

State Key Laboratory of Advanced Technology for Materials Synthesis and Processing, Wuhan University of Technology, Wuhan 430070, People's Republic of China

Received 4 December 2007; accepted 21 January 2008

DOI 10.1002/app.28438

Published online 12 August 2008 in Wiley InterScience (www.interscience.wiley.com).

**ABSTRACT:** The possibility of ultrathin Nafion/expanded polytetrafluoroethylene (ePTFE) membranes used as proton-exchange membranes (PEMs) for direct methanol fuel cells (DMFCs) was investigated in this study. Nafion/ePTFE membranes with a thickness of  $\sim 14 \mu\text{m}$  were promoted by self-assembling Pd nanoparticles on the surface to reduce the methanol crossover. The loading of the Pd nanoparticles assembled on the membranes was  $1.6\text{--}1.8 \mu\text{g}/\text{cm}^2$  and had little effect on the high conductivity of the Nafion membranes. With the self-assembly of Pd nanoparticles, the methanol permeation noticeably de-

creased from  $340$  to  $28 \text{ mA}/\text{cm}^2$ . As a result, the open-circuit voltage of the Nafion/ePTFE membranes that were self-assembled for 48 h had a more significant increase from  $0.55$  to  $0.73 \text{ V}$ . The reduction of methanol crossover significantly increased the DMFC voltage-current performance, and this means that self-assembled Nafion/polytetrafluoroethylene PEMs have promise in DMFCs. © 2008 Wiley Periodicals, Inc. *J Appl Polym Sci* 110: 2227–2233, 2008

**Key words:** metal-polymer complexes; polyelectrolytes

## INTRODUCTION

Direct methanol fuel cells (DMFCs) have the potential to power future microelectronic and portable electronic devices because of their high energy density and inherent simplicity of operation, with methanol as the liquid fuel. Compared to fuel cell systems using reformed  $\text{H}_2$  from methanol, DMFCs have the advantages of simple system design and cell operation.<sup>1,2</sup> Two major obstacles that currently prevent the widespread commercial applications of DMFCs are the low activity of the reported electrooxidation catalysts and the crossover of methanol through the proton-exchange membranes (PEMs).<sup>3,4</sup> It has been realized that methanol transported through PEMs will be oxidized at the cathode. Such an oxidation reaction lowers the cathode reactant. If a reaction intermediate, such as carbon monoxide, adsorbs onto the catalyst surface, the cathode will be poisoned too, and this will further lower its performance.<sup>5</sup>

Perfluorinated ionomer membranes are deemed the state of the art for electrolyte membranes in DMFC applications. A perfluorosulfonated acid polymer such as Nafion typically has  $\text{SO}_3^-$  side

chains fixed on the C–F backbones. Because of its structure, phase separation occurs between the hydrophilic and hydrophobic regions in hydrated Nafion.<sup>6,7</sup> Thus, hydrated protons can freely move through the channels produced by the phase separation, leading to high conductivity of the membranes. However, phase separation simultaneously provides channels for methanol and water molecules to pass through under the driving forces of concentration, pressure gradients, and electroosmosis. The development of ionomers with low methanol diffusivities without compromising the migration freedom of hydrated protonic clusters ions has proven to be very challenging.

One common approach for dealing with methanol crossover is the development of new proton-conducting membranes. The new polymers include polybenzimidazoles, polyamides, poly(ether imide)s, polysulfones, poly(phenylene sulfide)s, poly(ether ether ketone)s and polyphenylquinoxalines.<sup>8</sup> Nevertheless, Schaffer et al.<sup>9</sup> argued that even though these new types of polymer electrolytes reduce methanol crossover, they show low ionic conductivity.

Another approach is the modification of Nafion membranes to make them suitable for DMFC utilization. Jia et al.<sup>10</sup> impregnated Nafion membranes with poly(1-methylpyrrole) by *in situ* polymerization. The impregnation reduced the methanol crossover but also decreased the proton conductivity. Composite membranes such as sol-gel-derived Nafion/silica,<sup>11</sup>

Correspondence to: H. Tang (tanghaolin2005@yahoo.com.cn).

Nafion/zirconium phosphate,<sup>12</sup> and Nafion/cesium ion membranes<sup>13</sup> have also been investigated. To achieve a significant reduction in the methanol permeability, the oxide content has to be high (e.g., 20 wt % silica in the case of Nafion/silica composites<sup>11</sup>). This in turn affects the proton conductivity and other properties, such as the mechanical stability. Doping Nafion membranes with cesium ions reduces the methanol permeability, but the conductivity also decreases.<sup>14</sup> The use of Pd thin films sandwiched between Nafion membranes and the deposition of Pd nanoparticles through ion exchange and chemical reduction<sup>15</sup> have been shown to reduce methanol crossover. Unfortunately, the Pd films increase the overall cell resistance. The dispersed Pd particles through ion exchange and reduction affect the microstructure of the Nafion membranes, resulting in reduced cell performance and stability.

Nevertheless, most of the modifications have been based on pure Nafion membranes, which typically possess thicknesses greater than 50  $\mu\text{m}$  to maintain their mechanical strength. Previous reports have shown that a reduction of PEM thickness can be reached by the replacement of a pure Nafion membrane with a polytetrafluoroethylene (PTFE)-based composite membrane,<sup>16–21</sup> and this results in cost reduction and performance improvement. PTFE-based composite membranes are typically prepared by the impregnation of Nafion ionomers into porous PTFE [expanded polytetrafluoroethylene (ePTFE)] membranes. Because of their higher strength, the composite membranes can be used in fuel cells with a thinner thickness, and this results in higher area conductivity and the reduction of the amount of expensive Nafion resin needed. At the same time, the PTFE-enhanced structure significantly improves the membrane durability because freestanding pure Nafion ionomeric films are usually weak and susceptible to swelling in a hydrated state.<sup>22,23</sup>

For Nafion/ePTFE membranes, the proton-conducting resin, Nafion polymer, is accepted to have a dual structure with a hydrophobic region interspersed with ion-rich hydrophilic domains. Methanol diffuses primarily through the water-rich domains. It has been shown recently that selectively sealing water-rich domains on the surface of Nafion polymers, which are constructed of  $\text{SO}_3^-$  clusters, is a promising method for suppressing methanol crossover.<sup>24–26</sup> Pd nanoparticles should be able to block the  $\text{SO}_3^-$  sites without an adverse effect on the proton conductivity of Nafion membranes because Pd is highly permeable to hydrogen and capable of providing a methanol-blocking PEM. In this research, we investigate the methanol crossover behaviors of self-assembled Nafion/PTFE membranes and seek the possibility of adopting Nafion/PTFE membranes as potential DMFC PEMs.

## EXPERIMENTAL

### Synthesis of poly(diallyldimethylammonium chloride) (PDDA)-charged Pd particles

PDDA (20 wt % in water) with an average molecular weight of 5000 and  $\text{PdCl}_2$  (99.9%) were obtained from Aldrich. Low-molecular-weight PDDA was chosen to avoid multiparticle complexes (i.e., more than one Pd particle adsorbed onto one polymer molecule).<sup>17</sup> Milli-Q water (resistivity > 18.0  $\text{M}\Omega\text{ cm}$ ) was used in this work. Pd nanoparticles were prepared by the reduction of the metallic ions with EtOH alcohol (99.9%) in the presence of PDDA. A PDDA solution (0.002 mol/L) was put in a three-necked flask under intensive stirring for 10 min and then mixed with an appropriate amount of a  $\text{PdCl}_2$  solution (0.02 mol/L) for another 10 min; 60 mL of EtOH was added to the solution under continuous stirring. The pH of the solution was adjusted to 7.5 by the addition of NaOH. The solution was refluxed at  $\sim 84^\circ\text{C}$ .

### Preparation of the Nafion/ePTFE PEMs

The Nafion/ePTFE composite membrane was prepared as described in a previous work.<sup>16</sup> Before the preparation, 200 mL of Nafion ionomers (Nafion DE 520: 5 wt % Nafion,  $50 \pm 3$  wt % water, and  $48 \pm 3$  wt % 1-propanol; DuPont, Shanghai, China) was converted to the  $\text{Na}^+$  form by the slow addition of a solution of NaOH until the pH was 6.5–7.0. Ten milliliters of the nonionic surfactant Triton X-100 [poly(ethylene glycol)-*tert*-octylphenyl ether; Aldrich] was then added to the Nafion solution under continuous stirring. For the membrane preparation, a porous PTFE matrix (Shanghai Dagong Co., Shanghai, China; 85% porosity, pore size = 0.1–0.2  $\mu\text{m}$ ) was mounted on a 15 cm  $\times$  15 cm plastic frame and placed into a vacuum chamber. After the pressure of the vacuum chamber reached  $5 \times 10^2$  Pa, the Nafion/Triton-100 solution was pumped into the vacuum chamber to immerse the porous PTFE membrane in the Nafion solution for 150 s. Then, the vacuum chamber was opened to the ambient pressure. The impregnated PTFE membrane was then heat-treated at  $270^\circ\text{C}$  for 2 min to remove the solvent and induce the crosslinking of the Nafion ionomer. The impregnation and heat-treatment steps were repeated 3 times to reduce the voids in the composite membrane. The as-prepared composite membranes were immersed in distilled water for 24 h and in isopropyl alcohol for 5 min to remove Triton X-100, and this was followed by washing with distilled water. Finally, the membrane was treated in 0.5M sulfuric acid for 4 h and in distilled water for another 4 h. The thickness of the composite membranes was in general 14  $\mu\text{m}$ , and the prepared

membranes were called Nafion/ePTFE composite PEMs.

### Preparation of the self-assembled PEMs

The Nafion/ePTFE membrane (thickness = 13  $\mu\text{m}$ ) and the as-compared Nafion 112 membrane (thickness = 51  $\mu\text{m}$ ) were treated according to the standard procedure of 5 wt %  $\text{H}_2\text{O}_2$  for 0.5 h, 0.5 mol of  $\text{H}_2\text{SO}_4$  for 0.5 h, and distilled water for another 0.5 h. The self-assembly of Pd nanoparticles was carried out by the immersion of the pretreated membrane in water-dispersed Pd nanoparticles at room temperature. The pH of the solution was adjusted to 8.5 by the addition of NaOH. Then, the self-assembled membrane was recovered to the  $\text{H}^+$  form by a treatment in an 8 wt %  $\text{H}_2\text{SO}_4$  solution at 80°C for 30 min, and this was followed by rinsing in Milli-Q water at 80°C for 30 min.

### Instruments

Atomic adsorption analysis was employed to analyze the Pd loading of the self-assembled membrane through soaking in 2/3 HCl and 1/3  $\text{HNO}_3$  to dissolve Pd. The surface coverage of Pd nanoparticles on the Nafion membrane surface was calculated under the assumption of a spherical shape for the particles and a Pd density of 12.02  $\text{g}/\text{cm}^3$ . The proton conductivity of the PEMs was measured with a frequency response analyzer and a four-probe conductivity cell consisting of two platinum-wire outer current-carrying electrodes (distance = 3 cm) and two platinum-wire inner potential-sensing electrodes (distance = 1 cm) at 30°C. The methanol permeability of the Pd nanoparticle self-assembled membrane was measured with a diffusion cell consisting of two compartments separated by the membrane (area = 1  $\text{cm}^2$ ). One compartment of the cell contained a mixing solution of 2M MeOH, and the other compartment was filled with 1M sulfuric acid as the supporting electrolyte. Solutions in both cell compartments were stirred during the experiments. A polished, glassy carbon working electrode, a Pt foil counter electrode, and a saturated calomel electrode reference electrode were placed in the 1M sulfuric acid compartment. By the application of a dynamic potential to the working electrode, the limiting methanol oxidation current or crossover current, measured voltammetrically, was used as an indication of the methanol crossover rate.

A 40 wt % Pt-Ru/C catalyst (Pt/Ru atomic ratio = 1 : 1; Johnson Matthey, London, UK) with a loading of 1.6  $\text{mg}/\text{cm}^2$  was used in the anode. A 40 wt % Pt/C catalyst (Johnson Matthey) was employed as the cathode catalyst with a Pt loading of 1  $\text{mg}/\text{cm}^2$ . Catalyst inks were prepared and coated onto the

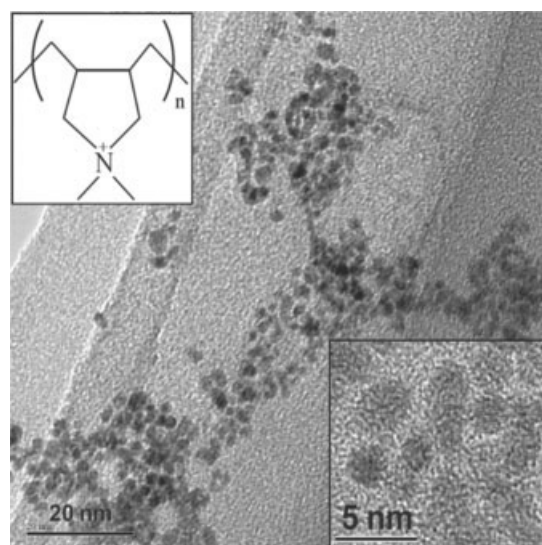


**Figure 1** TEM micrograph of as-prepared Pd nanoparticles. The molecular structure of PDAA is inset in the graph.

Teflon blanks. The catalyzed layer was then transferred onto the PEMs by the decal method. After that, the catalyzed membrane was hot-pressed between two carbon cloth diffusion electrodes to form the membrane-electrode assembly. The geometrical area of the electrodes was 4  $\text{cm}^2$ .

A PEFC test station (ElectroChem, United States) was used for the cell polarization testing. A 2 mol/L methanol solution was pumped through the DMFC anode at the flow rate of 6 mL/min with 0 psig back-pressure, and humidified oxygen was fed to the cathode at 150 mL/min with 0 psig back-pressure. The humidification temperature of the oxygen gas was 10°C lower than the cell operating temperature. The operating temperature of the cell was 60°C.

## RESULTS AND DISCUSSION

### Synthesis of the charged Pd nanoparticles

Figure 1 presents a transmission electron microscopy (TEM) micrograph of the Pd nanoparticles produced. The molecular structure of PDAA is also inset in the graph. The TEM image indicates the good dispersion of Pd nanoparticles, and the average particle size was 1.8 nm. The adsorbed PDAA stabilized the Pd nanoparticles by a combination of steric and electrostatic mechanisms. It is thought that the strong bonding between the particles and the polymer molecules, presumably through the interaction of the quaternary nitrogen atom with the metal, inhibited the agglomeration of Pd nanoparticles. The  $\zeta$  potential (determined with a  $\zeta$ -potential analyzer from ZetaPALS, Holtsville, NY) of the solution at a pH value of 8.5 was 30 mV, and this indicated that the



as-prepared Pd nanoparticles were indeed positively charged particles. The specific advantage of the positively charged nanoparticles was that they could be anchored to the sulfonic acid function group ( $-\text{SO}_3^-$ ) on the membrane surface. In particular, the diameter of the Pd particles was 1.8 nm, smaller than the size of the  $\text{SO}_3^-$  cluster (ca. 4 nm) but larger than the size of the  $\text{SO}_3^-$  cluster/bridge channels (ca. 1 nm).<sup>27,28</sup> This meant that the charged particles could be anchored onto the  $\text{SO}_3^-$  clusters on the Nafion polymer surface without entering the membrane.

### Preparation of the self-assembled PEM

The proton conductivity of membranes assembled for a specific time was measured to determine the  $-\text{SO}_3^-$  conditions. The assembled membranes were taken out from the  $\text{H}_2\text{O}$ -dispersed Pd nanoparticles and directly fixed in the four-point probe cell. After that, the membranes were recovered to the  $\text{H}^+$  form to measure the irreversible Pd loading on the assembled membranes. Shown in Figure 2(a) are the Pd loading of the assembled membranes (determined by atomic adsorption analysis) and the proton conductivity of the Nafion 112 membrane under the self-assembly procedure. The inset is the calculated Pd assembling rate from the Pd loading versus the time. The Pd loading on the Nafion membrane increased and the assembling rate decreased in the procedure until the balance reached about 48 h. The conductivity of the Nafion membrane decreased to 0.02 S/cm in the first 2 h and only slightly decreased in the next 70 h. This implies that the small ions, such as  $\text{Na}^+$  ions, possessed most of the  $-\text{SO}_3^-$  groups in the Nafion membrane because of their small scale and rapid thermal velocity. However, the fact that the Pd loading increased rapidly but the conductivity remained at  $\sim 0.02$  S/cm in 2–48 h reveals that an assembly–desorption dynamic balance existed, and the small cations were replaced by charged Pd particles until the Pd assembling balance was reached (ca. 48 h). The loading of the Pd nanoparticles assembled on the membrane was  $1.73 \mu\text{g}/\text{cm}^2$ . A further increase in the assembly time did not lead to a significant increase in the Pd loading, and this indicated the completion of the self-assembly of the Pd nanoparticles.

The self-assembled behavior of the Nafion/ePTFE membrane [Fig. 2(b)] was similar to that of the Nafion membrane. The Pd loading reached a balance with an assembly period of about 48 h, and the value was  $1.64 \mu\text{g}/\text{cm}^2$ . Because of the thickness difference between the Nafion membrane (51  $\mu\text{m}$ ) and the Nafion/ePTFE membrane (13  $\mu\text{m}$ ), the consistency of the Pd loading and self-assembly procedure also suggests that the Pd nanoparticles were assembled on the surface of the membrane.

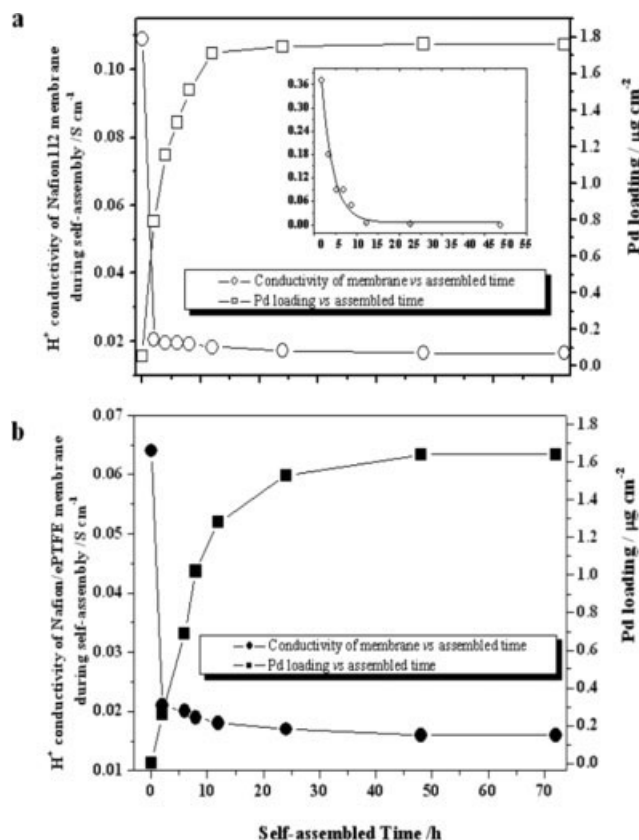


**Figure 2** Self-assembly Pd loading and proton conductivity of various PEMs as a function of the self-assembly time: (a) Nafion 112 membrane and (b) Nafion/ePTFE membrane.

The distribution or coverage of Pd nanoparticles assembled on the Nafion membrane can be estimated if we assume a monolayered structure and spherical shape of the Pd nanoparticles:

$$L_{Pd} = 2\rho \left( \frac{1}{d+l} \right)^2 \frac{2}{3} \pi \left( \frac{d}{2} \right)^3 \quad (1)$$

$$S_{Pd} = \pi \left( \frac{1}{d+l} \right)^2 \left( \frac{d}{2} \right)^2 \times 100\% \quad (2)$$

where  $L_{Pd}$  is the Pd loading,  $S_{Pd}$  is the surface coverage by Pd nanoparticles,  $d$  is the size of the Pd nanoparticles,  $l$  is the distance between Pd nanoparticles (edge to edge), and  $\rho$  is the density of Pd (12.02 g/ $\text{cm}^3$ ). The number 2 in the equation represents the two sides of the membrane. With  $d = 1.8$  nm and Pd loadings of 1.73 and  $1.64 \mu\text{g}/\text{cm}^2$  for the Nafion membrane and Nafion/ePTFE membrane, respectively, used to estimate the Pd nanoparticle distribution, the distance between Pd nanoparticles was  $\sim 0.26$  nm, and the surface coverage of the Pd nanoparticles on the Nafion membrane was 60%, and for the Nafion/ePTFE membrane, the distance between Pd nanoparticles was  $\sim 0.28$  nm, and the surface

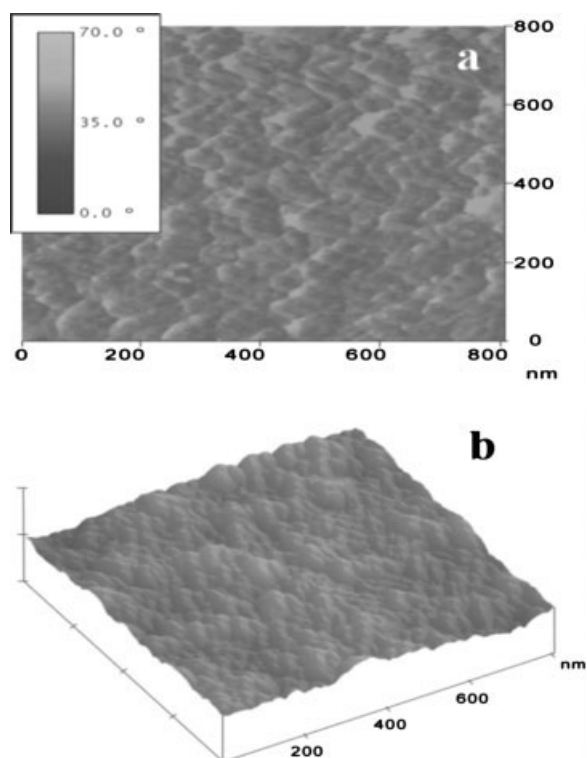


**Figure 3** Tapping-mode AFM micrographs of the 48-h self-assembled PEMs: (a) phase and (b) height.

coverage of the Pd nanoparticles on the Nafion membrane was 56%. This indicates that the self-assembled Pd nanoparticles most likely formed monolayer structures. An atomic force microscopy (AFM) micrograph (Nanoscope IIIa, Multimode, Santa Barbara, CA) of a polymer electrolyte membrane that was assembled for 48 h is shown in Figure 3. The Pd nanoparticles were dispersed uniformly on the Nafion surface. The average diameter of Pd particles was about 20 nm, a value considerably larger than the diameter of the Pd nanoparticles observed by TEM. Taking into account the thickness of the PDDA layer and convolution effects between the AFM tip and the sample, we found the differences in the diameters to be acceptable.<sup>29,30</sup> The energy dispersive X-ray (EDAX) mapping of the S and Pd elements on the self-assembled surface were also recorded in this research with a scanning electron microscopy (SEM) micrograph (Fig. 4). The results demonstrated the uniform distribution of the Pd nanoparticles.

**Performances of the self-assembled PEMs**

The PEMs assembled for various periods were recovered to H<sup>+</sup> to measure their methanol permeation current density and membrane area resistance. The limiting methanol permeation current densities of different PEMs were measured and are shown in Figure 5. The methanol crossover of the Nafion

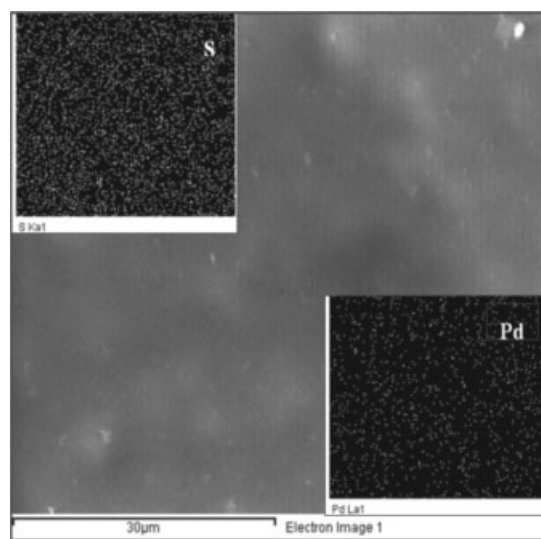


**Figure 4** Surface SEM micrograph of the 48-h self-assembled PEM. The inset pictures show corresponding EDAX S mapping of the S and Pd elements.

112 membrane decreased drastically from 150 to 20 mA/cm<sup>2</sup>, and this demonstrated the effective blocking of the sites for the methanol crossover

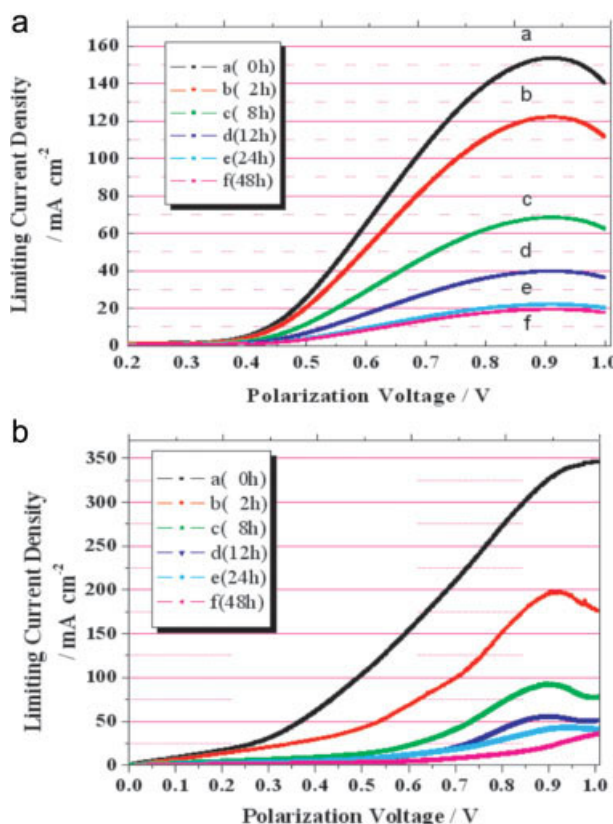


**Figure 5** Oxidation current of methanol migrating across the Pd nanoparticle PEMs as a function of the self-assembly time: (a) Nafion 112 membrane and (b) Nafion/ePTFE membrane. [Color figure can be viewed in the online issue, which is available at [www.interscience.wiley.com](http://www.interscience.wiley.com).]

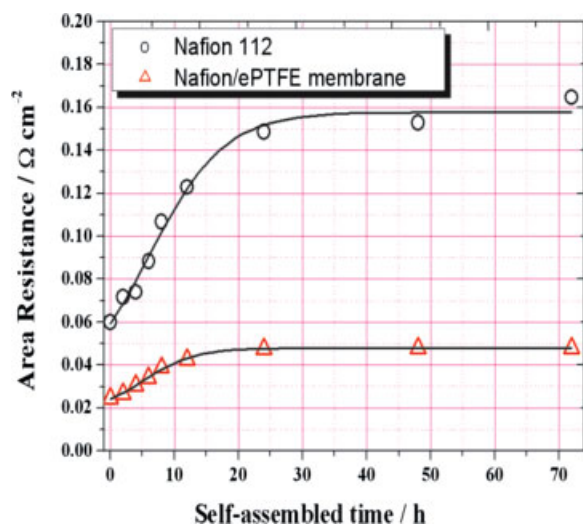


**Figure 6** Area resistance of Nafion 112 and Nafion/ePTFE membranes as a function of the self-assembly time. [Color figure can be viewed in the online issue, which is available at [www.interscience.wiley.com](http://www.interscience.wiley.com).]

through the self-assembly of the Pd nanoparticles at the membrane surface. The original Nafion/ePTFE membrane had a very large methanol crossover of 340 mA/cm<sup>2</sup>, probably because of the small thickness. With the self-assembly of Pd nanoparticles, the methanol permeation of the Nafion/ePTFE membrane noticeably decreased to 28 mA/cm<sup>2</sup>. Although the value was relatively high in comparison with the self-assembled Nafion membrane, the result was satisfactory when the membrane thickness was taken into account.

The resistances of the PEMs slightly increased with the introduction of self-assembly (Fig. 6). Relative selectivity for both the methanol crossover and resistance are also displayed in the figure. The relative selectivity ( $\alpha$ ) of the self-assembled PEMs was calculated from the methanol permeation current density and membrane area resistance with reference to a previous article:<sup>31</sup>

$$\alpha = \frac{R_N i_{\text{cross},N}}{R_S i_{\text{cross},S}} \quad (3)$$

where  $R_N$  and  $R_S$  are the area resistances for the pure Nafion and the self-assembled membrane, respectively, and  $i_{\text{cross},N}$  and  $i_{\text{cross},S}$  are the limiting methanol permeation current densities for the pure Nafion and the self-assembled membrane, respectively. At the self-assembly time of 48 h, the highest relative selectivity of 30 was achieved versus 1 for the original Nafion membranes. Compared to that of the Nafion 112 membrane, the relative selectivities of the original Nafion/ePTFE membrane and the 48-h self-assembled Nafion/ePTFE membrane were 10.6 and 71.4, respectively.

Current–voltage curves for single cells fabricated with various PEMs, as well as the open-circuit voltage (OCV), are displayed in Figure 7. The OCV of the fuel cell fabricated with self-assembled PEMs was clearly higher than that of a fuel cell fabricated with the original membrane. The value of the Nafion 112 membrane increased from 0.65 (pure Nafion 112) to 0.79 V (self-assembled for 48 h) as a function of the self-assembly time. For the Nafion/ePTFE membrane, the OCV of the membrane assembled for 48 h more significantly increased from 0.55 to 0.73 V. The change in the OCV<sup>32</sup> also revealed the blocking of the methanol crossover by the self-assembly of Pd nanoparticles. The thermodynamic reversible potential for a methanol–oxygen fuel cell is 1.45 V at 25°C. However, in practice, a DMFC has a much lower OCV. One of the major reasons is that methanol can cross through the PEM to reach the cathode side via physical diffusion and electroosmotic drag. Methanol crossover makes the potential of the cathode decrease from an oxygen reduction potential to a mixed potential of oxygen reduction and methanol electrooxidation, and this will lower the OCV of a DMFC single cell.<sup>29,30</sup> The current–voltage curves also show there was a lower slope in the intermediate density region (the so-called ohm polarization region) with Pd self-assembly versus that with the original PEM. However, the membrane resistance in Figure 6 indicates that the resistance increased with the increase in the Pd loading. The apparent contradiction can be reasonably attributed to the increase in the electroosmotic drag. The methanol crossover increased with the increase in the current density because of an increase in the electroosmotic drag, as reported in other articles.<sup>33</sup> As a result, the

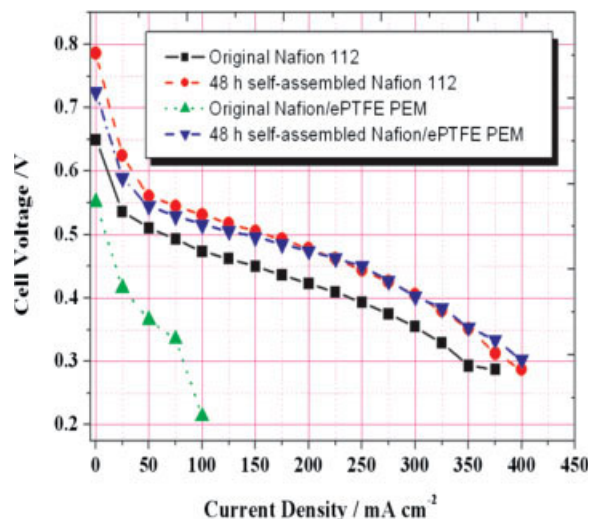


**Figure 7** Voltage-current performance of the original PEMs and the self-assembled PEMs. [Color figure can be viewed in the online issue, which is available at [www.interscience.wiley.com](http://www.interscience.wiley.com).]



self-assembled PEMs had better output than the pure PEMs. The figure also reveals that the self-assembled Nafion membrane had a larger OCV than the self-assembled Nafion/ePTFE membrane. However, the voltage reduction rate of the former was rapider than that of the latter. This demonstrated that the self-assembled Nafion/ePTFE membrane had superior proton conductance.

## CONCLUSIONS

A Nafion/ePTFE membrane was improved to meet the requirements of DMFC use through the self-assembly of charged Pd nanoparticles. Charged Pd nanoparticles were prepared through the refluxing of a solution of chloroplatinic acid and protective cationic agents (PDDA) in ethanol/water. The Pd nanoparticles showed a higher  $\zeta$  potential of 30 mV and a smaller size of about 1.8 nm. The charged Pd nanoparticles were self-assembled onto the PEM surface, and the assembly procedure was completed in about 48 h. The loading of the Pd nanoparticles assembled on the membrane was 1.6–1.8  $\mu\text{g}/\text{cm}^2$  and had little effect on the high conductivity of the Nafion membrane. With the self-assembly of the Pd nanoparticles, the methanol permeation noticeably decreased from 340 to 28  $\text{mA}/\text{cm}^2$ . As a result, the OCV of the Nafion/ePTFE membrane that self-assembled for 48 h more significantly increased from 0.55 to 0.73 V. The reduction of methanol crossover also increased the DMFC voltage-current performance, and this gives self-assembled Nafion/PTFE PEMs potential in DMFCs.

## References

1. Deluca, N. W.; Elabd, Y. A. *J Polym Sci Part B: Polym Phys* 2006, 44, 2201.
2. Song, S. Q.; Tsiakaras, P. *Appl Catal B* 2006, 63, 187.
3. Kamarudin, S. K.; Daud, W. R. W.; Ho, S. L.; Hasran, U. A. *J Power Sources* 2007, 163, 743.
4. Du, C. Y.; Zhao, T. S.; Yang, W. W. *Electrochim Acta* 2007, 52, 5266.
5. Curau, B.; Smotkin, E. S. *J Power Sources* 2002, 112, 339.
6. Paddison, S. J.; Elliott, J. A. *Phys Chem Chem Phys* 2006, 8, 2193.
7. Doyle, M.; Rajendran, G. In *Handbook of Fuel Cells*; Wiley: Chichester, England, 2003; Vol. 3, p 351.
8. Kerres, J. A. *J Membr Sci* 2001, 185, 3.
9. Schaffer, T.; Hacker, V.; Hejze, T.; Tschinder, T.; Besenhard, J. O.; Prenninger, P. *J Power Sources* 2005, 145, 188.
10. Jia, N.; Lefebvre, M. C.; Halfyard, J.; Qi, Z.; Pickup, P. G. *Electrochem Solid-State Lett* 2000, 3, 529.
11. Miyake, N.; Wainrigh, J. S.; Favinnell, S. R. *J Electrochem Soc* 2001, 148, A905.
12. Yang, C.; Srinivasan, S.; Aricò, A. S.; Creti, P.; Baglio, V.; Antonucci, V. *Electrochem Solid-State Lett* 2001, 4, A31.
13. Tricoli, V. *J Electrochem Soc* 1998, 145, 3798.
14. Pu, C.; Huang, W.; Ley, K. L.; Smotkin, E. S. *J Electrochem Soc* 1995, 142, L119.
15. Kim, Y. J.; Choi, W. C.; Woo, I.; Hong, S. W. H.; Shen, P. K.; Jiang, S. P. *J Phys Chem B* 2007, 111, 8684.
16. Tang, H. L.; Wang, X. E.; Pan, M.; Wang, F. *J Membr Sci* 2007, 306, 298.
17. Bahar, B.; Hobson, A. R.; Kolde, J. U.S. Pat. 5,547,551 (1996).
18. Liu, W.; Ruth, K.; Rusch, G. *J New Mater Electrochem Sys* 2001, 4, 227.
19. Lin, H.; Yu, T.; Shen, K.; Huang, L. *J Membr Sci* 2004, 237, 1.
20. Ramya, K.; Velayutham, G.; Subramaniam, C. K.; Rajalakshmi, N.; Dhathathreyan, K. S. *J Power Sources* 2006, 160, 10.
21. Huang, X. Y.; Solasi, R.; Zou, Y.; Feshler, M.; Eifsnider, K.; Condit, D.; Burlatsky, S.; Madden, T. *J Polym Sci Part B: Polym Phys* 2006, 44, 2346.
22. Tang, H. L.; Shen Peikang, P. K.; Jiang, S. P.; Wang, F.; Pan, M. *J Power Sources* 2007, 170, 85.
23. Tang, H. L.; Pan, M.; Wang, F.; Shen, P. K.; Jiang, S. P. *J Phys Chem B* 2007, 111, 8684.
24. Jiang, S. P.; Liu, Z. C.; Tian, Z. Q. *Adv Mater* 2006, 18, 1068.
25. Tang, H. L.; Pan, M.; Jiang, S. P.; Wan, Z.; Yuan, R. Z. *Colloids Surf A* 2005, 262, 65.
26. Tang, H. L.; Pan, M.; Jiang, S. P.; Yuan, R. Z. *Mater Lett* 2005, 59, 3766.
27. Yeager, H. L.; Kipling, B. *J Phys Chem* 1979, 83, 1836.
28. Orfino, F. P.; Holdcroft, S. *J New Mater Electrochem Sys* 2000, 3, 285.
29. Grabar, K. C.; Brown, K. R.; Keating, C. K.; Stranick, S. J.; Tang, S.; Natan, M. J. *Anal Chem* 1997, 69, 471.
30. Peng, Z.; Qu, X.; Dong, S. *Langmuir* 2004, 20, 5.
31. Libby, B.; Smyrl, W. H.; Cussler, E. L. *Electrochem Solid-State Lett* 2001, 4, A197.
32. Hikita, S.; Yamane, K.; Nakajima, Y. *JSAE Rev* 2001, 22, 151.
33. Kho, B. K.; Bae, B.; Scibioh, M. A.; Lee, J.; Ha, H. Y. *J Power Sources* 2005, 142, 50.